RESEARCH ARTICLE

MIGRATION STRUCTURES OF MEANDERING CHANNELS

[1,2]Zhipeng Lin, *,[1,2]Jingfu Shan, [1,2]Le Chen, [3]Qianjun Sun and Yiwu Wang

[1]Key Laboratory of Exploration Technologies for Oil and Gas Resources, Ministry of Education, Yangtze University, Wuhan 430100, China
[2]School of Geosciences, Yangtze University, Wuhan 430100, China
[3]School of Energy Resources, China University of Geosciences, Beijing 100083, China
[4]School of Earth and Space Sciences, Peking University, Beijing 100871, China

ARTICLE INFO	ABSTRACT
	The migration structure is the foundation of the restoration for the sedimentary evolution of paleochannel, as well as the base for predicting the tendency of the migration. It is the aims of this paper to reveal the migration structures of a meandering channel by using the historical satellite images and observation data from the technique of Google Earth and ACME Mapper. The target river is Irtysh River, which is free from the impact of human being, thus making the preservation condition of the structure of this natural channel is relatively good. 50 meanders of this river are investigated and 6 of them are chosen for detailed characterization. During the process, static elements and dynamic elements are adopted to demonstrate the plane structure of the meandering channel. Simultaneously, 5 kinds of parameters are proposed to quantitatively reveal the structure of channel. Extraordinarily, 3 of them are firstly posed and the other two are also different with the definition of predecessors. Through the meticulous analysis for the migration structures of 6 typical meander loops, 6 kinds of basic planform structures of migration are obtained. Eventually, 9 migration patterns of the meandering channel are concluded.

INTRODUCTION

The evolution of the geomorphic structure of a fluvial, especially the meandering channel, obviously plays a vital role in controlling the lithology and reservoir of the stratigraphic properties(Kasvi 2015; Shan *et al.* 2015). Reconstruction of the meandering process of a channel depends on the understanding of the planform migration structure. However, this theory is still now relatively insufficient(Ma *et al.* 2008). The understanding of the migration structure of the meandering channel is the core to determinate the sedimentary course of the ancient river(Blum *et al.* 2013; Schuurman *et al.* 2016; Kasvi *et al.* 2017; Lin *et al.* 2017). By means of discovering the discipline of the channel structure, comprehending with the distribution characteristics of underground sand bodies will surely be easier (Sui 2006; Willis and Tang 2010; Mithun *et al.* 2012; Asahi *et al.* 2013; Hu *et al.* 2017).

Moreover, the structure of the internal sand body is very complex and the traditional method is difficult to accurately characterize the reservoir architecture of the underground unit (Nami 1976; Xue 1991; Wu and Wang 1999; Mu 2000; Yin *et al.* 2001; Hu 2016; Hu *et al.* 2017). Although an increasing amount of literature focus on the ancient and modern fluvial system, the geomorphological process of meandering evolution remains a problem (Zhang *et al.* 2004; Willis and Tang 2010; Ielpi and Ghinassi 2014; Debnath *et al.* 2017). Currently, researchers around the world have begun to develop the analysis of migration evolution structure of meandering rivers. The models of the translation, rotation, and expansion of meanders that proposed before needs further explore (Brice 1974; Jackson 1976; Hooke 1980; Hooke 1984; Gilvear *et al.* 2000). Obvious results such as (Ghinassi *et al.* (2014); Ielpi and Ghinassi (2014), through the researches for the morphology of the meandering bend in northern Scarborough, Yorkshire, United Kingdom, Ielpi and Ghinassi proposed a comprehensive model of facies distribution. Wu *et al.*(2015; 2016) analyzed the evolution of channel sediments by reconstructing the migration pattern of composite point bars from outcrop and examining ancient exhumed channel belts, eventually established a semi-quantitative channel migration model;

*Corresponding author:[1,2]Jingfu Shan,
[1]Key Laboratory of Exploration Technologies for Oil and Gas Resources, Ministry of Education, Yangtze University, Wuhan 430100, China.
[2]School of Geosciences, Yangtze University, Wuhan 430100, China.

Ghinassi *et al.*(2014; 2016) focused on the planform evolution and stratal architecture of the meandering channel and discussed it as an important method to reconstruct the palaeoflow and facies distribution and develop the fluvial hydrocarbon reservoirs. Schuurman *et al.*(2016) observed the morphological changes and migration of meandering river by establishing morphological numerical model experiments. Thus it can be seen this topic that it is necessary to understand the process of the evolution of the planform migration architecture of meandering river.

The purpose of this paper is to explore the planform migration architecture of meandering rivers and the basic rules and models. By means of high-resolution historical satellite images from Google Earth and ACME Mapper (A kind of software based on Google Earth), the research characterizes on Irtysh River, which is relatively in the considerable preservation condition of the natural architecture and free from the impact of human beings.

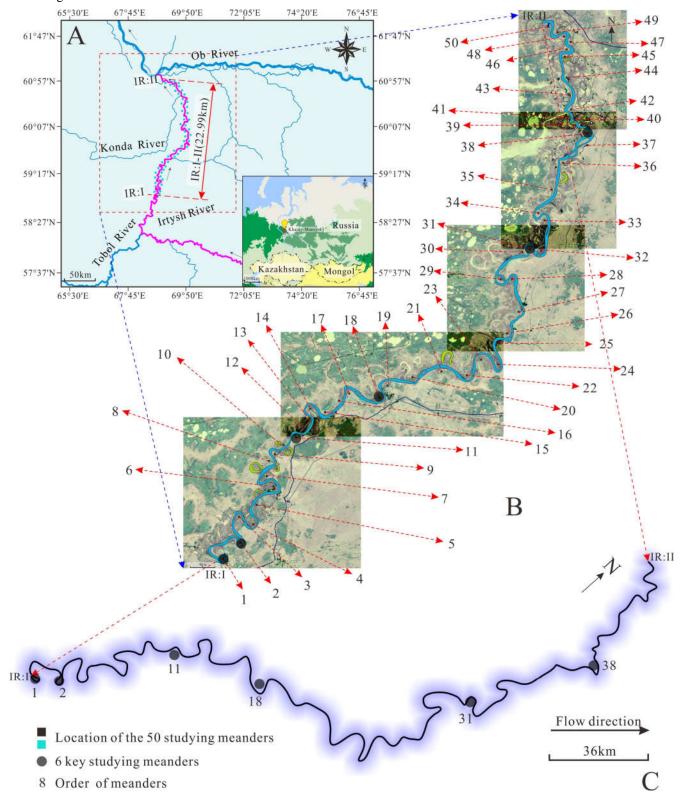**Figure 1. Location map of the Irtysh River: A 50 meanders are investigated in reach IR: I-II, coordinate information comes from Google Earth and ACME Mapper. B the details of the 50 studying meanders in the composite satellite images of Google Earth, showing the orders of the meanders. C extracted centerline(see Figure 2) from the research drainage area of the Irtysh River, marked the 6 key studying meanders**
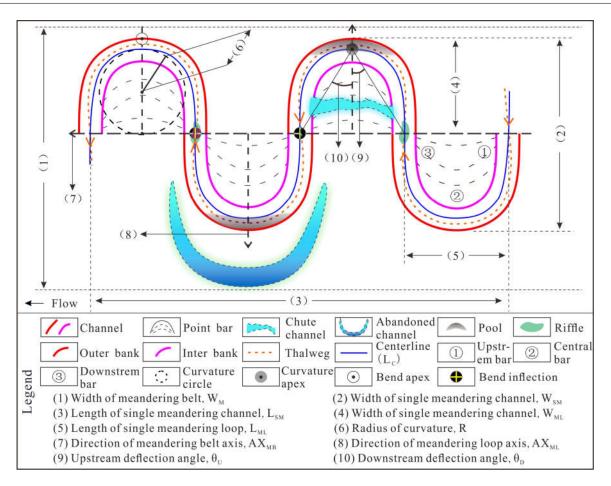
Figure 2. The idealized meandering migration architecture model, which includes 17 static elements and 12 dynamic elements

Table 1. The Planform Architecture Elements and Parameters of the 6 Key Studying Meanders in the reach IR: I-II

Elements	Irtysh River					
Meander	1	2	11	18	31	38
Latitude	58°52'N	58°56' N	59°20' N	59°34' N	60°14' N	60°40' N
Longitude	68°47'E	68°50'E	68°52'E	69°17'E	69°48'E	69°52'E
W_M/m	16520.9	14479.6	13068.9	14855.1	10522.0	22592.7
L_M/m	302741	302741	302741	302741	302741	302741
W_{SM}/m	12263.0	9765.0	2467.3	12230.8	7394.3	13075.5
L_{SM}/m	11094.8	11813.2	8409.4	23525.6	17068.8	18441.5
W_{ML}/m	3821.3	2541.6	1758.1	3225.5	2642.6	3309.8
L_{ML}/m	919.7	2472.9	3551.9	7637.9	2282.7	3145.0
L_C/m	10166.9	7305.9	4626.3	11994.3	6999.2	6315.5
R/m	2155.3	1389.6	729.7	2148.5	1318.1	1311.9
$|AX_{MB}|$/m	919.7	2472.8	3551.9	7637.9	2282.7	3145.0
AX_{MB}/°	344.3	103.7	211.8	226.9	49.7	336.5
AX_{ML}/°	44.0	136.9	311.9	94.4	316.8	110.1
θ_U/°	9	20	50	18	30	34
θ_D/°	12	13	55	55	28	15
S	11.05	2.95	1.30	1.57	3.07	2.01
C	0.0005	0.0007	0.0014	0.0005	0.0008	0.0008
$\Delta\theta$/°	-3	7	-5	-37	2	19
$\Delta\theta'$/°	3	-7	5	37	-2	-19
K_M	0.22	0.89	2.43	1.78	0.87	1.20

Note: W_M: width of meandering belt, L_M: length of meandering belt, W_{SM}: width of single meandering channel, L_{SM}: length of single meandering channel, W_{ML}: width of single meandering loop, L_{ML}: length of single meandering loop, L_C: length of channel centerline, R: radius of curvature, $|AX_{MB}|$: length of meandering belt axis, AX_{MB}: direction of meandering belt axis, AX_{ML}: direction of meandering loop axis, θ_U: upstream deflection angle, θ_D: downstream deflection angle, S: sinuosity index, C: curvature, $\Delta\theta$: difference of along-current deflection angle, $\Delta\theta'$: difference of counter-current deflection angle, K_M: expansion coefficient.

For these targets, we will try to characteristic the morphological elements of planform architecture of meandering rivers and understand the geomorphology process and migration characteristics of different meandering channels.

MATERIALS AND METHODS

The paper picks the Irtysh River as the target object of study and numbered 50 meanders for investigation, among them, 6 are utilized for a detailed description. The reason for selecting

Irtysh River is that the channel structure of meandering is preserved relatively in good condition and easier to observe. The Irtysh River is one of the largest tributaries of the Ob River, which is about 4248 km long and flows from the southeast to the northwest of the Altai Mountains, Xinjiang, China, flows via Kazakhstan North into Russia, in the Khanty-Mansysky importing into the Ob River. The study area lies from the north of Tobolsk, with coordinates of 60°56'N and 69°19'E, as shown in Figure 1, for reach IR: I-II, with a length of 44.51 km and a straight line distance of 22.99 km.

Basic elements

The meandering structure is the basis for depicting the migration process of channels. Currently, the description and characterization of morphology structure of modern alluvial plain are still limited to the interpretation of microfacies (He and Wang 2008; Zhu 2008; Feng 2013; Xu *et al*. 2016). Methods here are shown by employing basic elements of planform architecture of meandering channel with a new perspective. Based on the investigatory of the structure international researches(Brice 1974; Willis and Tang 2010; Mithun, Dabojani *et al*. 2012; Wu, Ullah *et al*. 2016; Fryirs 2017; Kasvi, Laamanen *et al*. 2017), we propose the characterization elements of meandering migration architecture with systematic examination, Overall, the basic elements are divided into 2 parts: static elements and dynamic elements. The static elements refer to the geomorphic deposition unit and the abstract concept streamline which can be adopted to describe qualitatively the plane structure of the meandering river (Figure 2). It mainly includes the in-channel elements: main channel, pool, riffle, thalweg, centerline, bend inflection, and curvature apex. And the outbank elements are: meandering belt, point bar (upstream bar, central bar, downstream bar), chute channel, outer bank (concave bank), the inner bank (convex bank), meandering loop (meander or bend), abandoned channel, floodplain(overbank), curvature circle, and bend apex. Among them, the major elements for plane migration structure characterization are the following ones like a meandering loop, centerline, bend inflection, curvature apex, curvature circle, point bar, and thalweg. The dynamic elements refer to the quantitative parameter extracted from the static elements, which is the quantitative reflection and presentation of the channel structure. The numerical change can indicate the migration architecture of the meandering river to a certain extent. It mainly include scalar element and vector element, the former includes: width of meandering belt (W_M), length of meandering belt (L_M), width of single meandering channel (W_{SM}), length of single meandering channel (L_{SM}), width of single meandering loop (W_{ML}), length of single meandering loop(L_{ML}), length of channel centerline(L_C), and radius of curvature(R). While the latter includes: meandering belt axis (AX_{MB}), meandering loop axis (AX_{ML}), upstream deflection angle (θ_U), and downstream deflection angle (θ_D), (Table 1, Figure 2).

Characterization parameters

The basic elements are representative of the characteristics of the channel structure, however, in order to quantify the characteristics of the migration architecture, structural elements for the dynamic evolution of meandering process need to do feature analysis, that is, characterization parameters. According to the structural elements above, five characterization

parameters are extracted: sinuosity index (S), curvature (C), difference of along-current deflection angle ($\Delta\theta$), difference of counter-current deflection angle ($\Delta\theta'$), and expansion coefficient (K_M), in which the parameters of $\Delta\theta$, $\Delta\theta'$ and K_M are presented with a tentative for the first time in this paper while the parameters of S and C is also demonstrated with a new idea. The basic elements and characterization parameters of the river segment are shown in Table 1. Sinuosity index (S) refers to the ratio of the length of centerline to the corresponding meandering belt axis, which is adoped to indicate the bending degree. The definition of the sinuosity previously is the ratio of the length of the channel to the valley. However, evidently, the problem is that how to understand the definition of the length channel, valley, outer bank line, interbank line, thalweg, and centerline, or the length of the straight line of the starting and ending points of the river. The distinction is not clear enough that the characterization of sinuosity is likely to cause confusion. Nevertheless, with this new definition, using the length of the centerline to represent the length of a river, the confusion of channel length can get unified. Simultaneously, the utilization of the length of meandering belt axis instead of length of valley, on the one hand, will not cause the fuzzy of concept; On the one hand, as mentioned earlier, the length of meandering belt axis rather than the straight distance from the beginning to the end point could accurately reflect the sinuosity situation, since it takes into account the migration of channel morphology with the terrain meandering factors, rather than simplifying the distance as a straight line. Expressed as a formula can be written:

$$S = L_C / \left| AX_{MB} \right| \qquad (3\text{-}1)$$

Curvature (C) refers to the reciprocal of curvature radius (R) of corresponding research meander, which is taken to indicate the degree and scale of a meander. The greater the curvature is, the greater the degree of the channel bending is. The method of calculating curvature according to the ratio between the arc length and the diameter of a point bar(Shi *et al*. 2012) has a certain degree of ambiguity because the extracted diameter and the arc length from the irregularity of the point bar are not clear for lack of accurate definition. Here the choice of R is of great concern, which is not a simple half of the so called diameter of a point bar. Firstly, through the two bend inflections one can determine the starting and end point of the meander. Secondly, define the curvature apex and control the shape of the entire meandering loop. Ultimately, through these three points: two bend inflections and one curvature apex, the thus obtained curvature circle and R could be an effectively better representative for the truth of curvature. Expressed as the formula below:

$$C = 1 / R \qquad (3\text{-}2)$$

The difference of along-current deflection angle ($\Delta\theta$) refers to the difference between the upstream deflection angle (θ_U) and downstream deflection angle (θ_D), reflecting the symmetry of a bend. The closer the value is to 0, the higher the symmetry of the meandering loop is. Moreover, while the value is positive and greater, the curvature apex is indicated closer to the upstream bend inflection, showing a tendency of counter-current rotation.
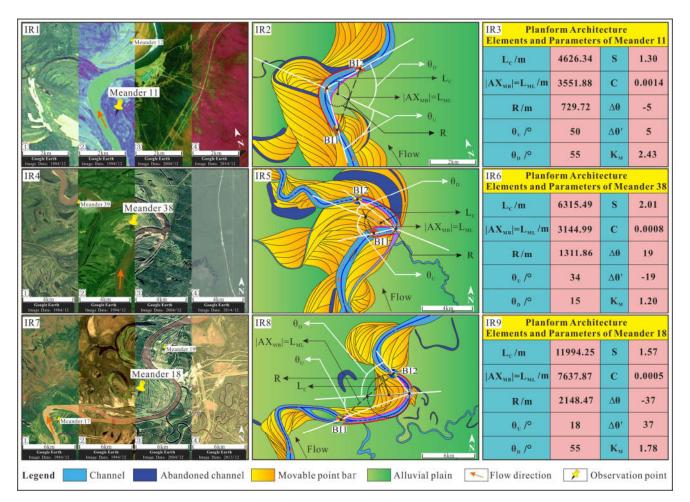
Figure 3. Planform migration architecture of the Expansion Structure of the Irtysh River: IR1-IR3 is the performance of Symmetrical Expansion Structure in meander 11, while IR1 shows the satellite images taken in the last 30 years and coordinates are 59°20'N and 68°52'E; IR2 shows the planform migration architecture in details, and IR3 shows the statistical data of planform migration architecture elements and parameters of meander 11. IR4-IR6 is the performance of Upstream Rotation Expansion Structure in meander 38, while IR4 shows the satellite images taken in the last 30 years and coordinates are 60°40'N, 69°52'E; IR5 shows the planform migration architecture in details, and IR7 shows the statistical data of planform migration architecture elements and parameters of meander 38. IR7-IR9 is the performance of Downstream Rotation Expansion Structure in meander 18, while IR7 shows the satellite images taken in the last 30 years and coordinates are 64°45'N, 154°20'E; IR8 shows the planform migration architecture in details, and IR9 shows the statistical data of planform migration architecture elements and parameters of meander 18. Images and coordinates information come from Google Earth and ACME Mapper.

On the contrary, the difference is negative and smaller, the curvature apex is indicated closer the downstream bend inflection, showing a tendency of along-current rotation. Formula is:

$$\Delta\theta = \theta_U - \theta_D \qquad (3\text{-}3)$$

Meanwhile, contrary to $\Delta\theta$, the $\Delta\theta'$, difference of counter-current deflection angle, refers to the difference between the downstream deflection angle (θ_D) and upstream deflection angle (θ_U), with objective similarity and perspective diversity. The closer the value is to 0, the higher the symmetry of the meandering loop is. While the value is positive and greater, the curvature apex is indicated closer to the downstream bend inflection, showing a tendency of along-current rotation. On the contrary, the difference is negative and smaller, the curvature apex is indicated closer the upstream bend inflection, showing a tendency of counter-current rotation. Write as:

$$\Delta\theta' = \theta_D - \theta_C \qquad (3\text{-}4)$$

Expansion coefficient (K_M) refers to the ratio of the length of single meandering loop (L_{ML}) to the diameter of curvature circle ($2R$). Basically, this coefficient could represent the changes of meandering shape because it is dominated by the elements of both bend reflection and curvature apex. When the meandering loop migrates outward with expansion, the curvature diameter ($2R$) tends to be generally larger with the control of bend reflection, while the length of single meandering loop relatively changes less. Thus the value of K_M decreases gradually to 1. When the meander expands to a certain extent, constriction process begins. Within the course, the curvature diameter is generally going to be larger than the length of the single meandering loop, leading to the value of K_M decreases to less than 1. This is the course of how the K_M could quantitatively reflect the situation of expansion and constriction process of a channel. See as a formula:

$$K_M = L_{ML} / 2R \qquad (3\text{-}5)$$

RESULTS

With this study, there were 50 subjects and 6 cases are conducted with the quantitative study of the meandering channel with the basic and characterization parameters. Meanwhile, the migration structures of the channel in the Irtysh River are followed by the expansion and constriction structures, which is demonstrated as below:

Expansion structure

According to the swing difference of meandering loops and point bar and the value of $\Delta\theta$ and $\Delta\theta'$, the expansion structure can be specifically subdivided into 3 parts (Figure 3): Symmetrical Expansion Structure, Upstream Rotation Expansion Structure, and Downstream Rotation Expansion Structure.

The meandering loop continuously erodes the outer banks and the symmetry is good, K_M is greater than 1 and $\Delta\theta$ is close to 0°, this is the Symmetrical Expansion Structure. As shown in Figure 3 IR1-IR3, IR1 shows the satellite images of meander 11 from years 1984 to 2014, the migration of bend 11 is not obvious. Through the planform migration architecture of IR2 and characterization parameters of IR3, we can see that the value of S is 1.3, C is 0.0014, reflecting that the bending degree is in general; $\Delta\theta$ is -5° and $\Delta\theta'$ is 5°, indicating that the symmetry of the meander is relatively better with a slight trend of along-current rotation. K_M is 2.43, indicating that the river is in the expansion period, and the degree of expansion is small.

The meandering loop continuously erodes the outer banks with curvature apex being closer to the upstream bend inflection, showing a tendency of counter-current rotation, K_M is greater than 1 and $\Delta\theta$ is positive, this is the Upstream Rotation Expansion Structure. As shown in Figure 3 IR4-IR6, IR4 shows that from years 1984 to 2014, the migration of the meander 38 in the Irtysh River is weak.

Through the planform migration architecture of IR5 and characterization parameters of IR6, it can be seen that the value of S is 2.01, C is 0.0008, reflecting a greater degree of bending; $\Delta\theta$ is 19° and $\Delta\theta'$ is -19°, indicating that the curvature apex is closer to the upstream bend inflection with the tendency of counter-current rotation. K_M is 1.20, indicating that the river bend is in the expansion period with a greater degree. The meandering loop continuously erodes the outer banks with curvature apex being closer to the downstream bend inflection, showing a tendency of along-current rotation, K_M is greater than 1 and $\Delta\theta$ is negative, this is the Downstream Rotation Expansion Structure. As shown in Figure 3 IR7-IR9, IR7 shows that from years 1984 to 2013, the migration process is slow, and it is shown that value of S is 1.57 and C is 0.0005 by the planform migration architecture of IR8 and characterization parameters of IR9, reflecting a greater degree of bending; $\Delta\theta$ is -37° and $\Delta\theta'$ is 37°, indicating that the curvature apex is closer to the downstream bend inflection with the tendency of along-current rotation. K_M 1.78, indicating that the river is in the expansion period with a greater degree.

Constriction structure

According to the swing difference of meandering loops and point bar and the value of $\Delta\theta$ and $\Delta\theta'$, the constriction structure can also be specifically subdivided into 3 parts (Figure 4): Symmetrical Constriction Structure, Upstream Rotation Constriction Structure, and Downstream Rotation Constriction Structure.

The process of outward expansion of the meandering loop slows down and the symmetry is maintained, and the trend of cut-off is starting gradually near the bend inflections. K_M is less than 1 and $\Delta\theta$ is close to 0°, this is the Symmetrical Constriction Structure. As shown in Figure 4 IR10-IR12, IR10 shows the satellite images of meander 31 from years 1984 to 2015, the migration of riverbed 31 is relatively slow. Through the planform migration architecture of IR11 and characterization parameters of IR12, it can be seen that the value of S is 3.07, C is 0.0008, reflecting the higher bending degree; $\Delta\theta$ is 2° and $\Delta\theta'$ is -2°, indicating that the symmetry of the bend is relatively better with a slight trend of counter-current rotation. K_M is 0.87, revealing that the river is in the constriction period, and the degree of constriction is small. The process of outward expansion of the meandering loop slows down with curvature apex being closer to the upstream bend inflection, showing a tendency of counter-current rotation, and the trend of cut-off is starting gradually near the bend inflections. K_M is less than 1 and $\Delta\theta$ is positive, this is the Upstream Rotation Constriction Structure. As shown in Figure 4 IR13-IR15, IR13 shows that from years 1984 to 2016, the migration of the meander 2 in the Irtysh River is slow. Through the planform migration architecture of IR14 and characterization parameters of IR15, it can be seen that the value of S is 2.95, C is 0.0007, reflecting a greater degree of bending; $\Delta\theta$ is 7° and $\Delta\theta'$ is -7°, indicating that the curvature apex is closer to the upstream bend inflection with the tendency of counter-current rotation. K_M is 0.89, indicating that the meander is in the constriction period with a greater degree.

The process of outward expansion of the meandering loop slows down with curvature apex being closer to the downstream bend inflection, showing a tendency of along-current rotation, and the trend of cut-off is starting gradually near the bend inflections. K_M is less than 1 and $\Delta\theta$ is negative, this is the Downstream Rotation Constriction Structure. As shown in Figure 4 IR16-IR18, IR16 shows that from years 1984 to 2016, the migration process of the meander 1 is not clear, and it is shown that value of S is 11.05 and C is 0.0005 by the planform migration architecture of IR17 and characterization parameters of IR18, reflecting a greater degree of bending; $\Delta\theta$ is -3° and $\Delta\theta'$ is 3°, indicating that the curvature apex is closer to the downstream bend inflection with the tendency of along-current rotation. K_M 0.22, indicating that the river is in the constriction period with a greater degree.

DISCUSSION

Through the characterization and analysis of planform migration structure, it is worthy of discussion the migration model of meandering channel and investigation the process of the river bending. Combining with the characteristics of the above elements and parameters, the ideal models of meanders may be discussed and concluded below.

Expansion migration model

When the meandering channel continuously migrate laterally and the curvature apex is approximately shifting with linear

movement. The value of L_C, S, and R increases gradually, while the $|AX_{MB}|$ and L_{ML} remain relatively stable with the slow decrease, C decreases gradually; θ_U and θ_D remain constant, $\Delta\theta$ and $\Delta\theta'$ are basically maintained at 0°.

θ_D increases gradually, while the $|AX_{MB}|$ and L_{ML} remain relatively stable with the slow decrease, C, and θ_U decreases gradually; $\Delta\theta$ is negative and decrease gradually while $\Delta\theta'$ is positive and increases gradually.
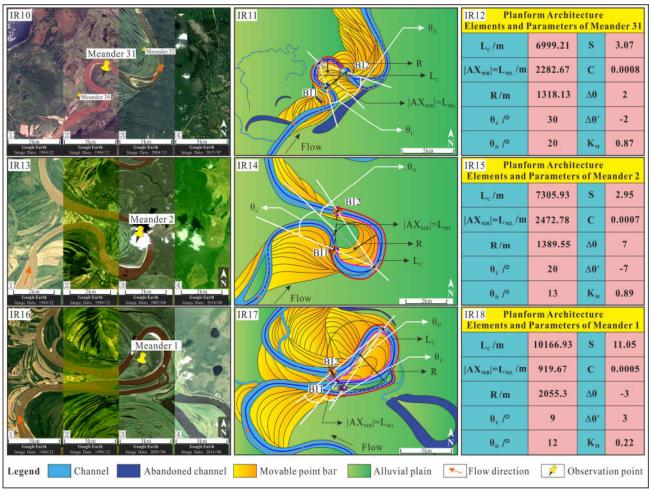

Figure 4. Planform migration architecture of the Constriction Structure of the Irtysh River: IR10-IR12 is the performance of Symmetrical Constriction Structure in meander 31, while IR10 shows the satellite images taken in the last 30 years and coordinates are 60°14'N, 69°48'E; IR11 shows the planform migration architecture in details; and IR12 shows the statistical data of planform migration architecture elements and parameters of meander 31. IR13-IR15 is the performance of Upstream Rotation Constriction Structure in meander 2, while IR13 shows the satellite images taken in the last 30 years and coordinates are 58°56'N, 68°50'E; IR14 shows the planform migration architecture in details, and IR15 shows the statistical data of planform migration architecture elements and parameters of meander 2. IR16-IR18 is the performance of Downstream Rotation Constriction Structure in meander 1, while IR16 shows the satellite images taken in the last 30 years and coordinates are 58°52'N, 68°47'E; IR17 shows the planform migration architecture in details, and IR18 shows the statistical data of planform migration architecture elements and parameters of meander 1. Images and coordinates information come from Google Earth and ACME Mapper

K_M is always greater than 1, this may be concluded as the meandering model of Symmetrical Expansion Migration. The meander 11 in IR1 (Figure 3) reveals this model. When the meandering channel continuously migrate laterally and the curvature apex is approximately shifting with the curvilinear movement towards the upstream. The value of L_C, S, R, and θ_U increases gradually, while the $|AX_{MB}|$ and L_{ML} remain relatively stable with the slow decrease, C, and θ_D decreases gradually; $\Delta\theta$ is positive and increases gradually while $\Delta\theta'$ is negative and decreases gradually.

K_M is always greater than 1, this may be concluded as the meandering model of Upstream Rotation Expansion Migration. The meander 38 in IR4 (Figure 3) reveals this model. When the meandering channel continuously migrate laterally and the curvature apex is approximately shifting with the curvilinear movement towards the downstream. The value of L_C, S, R, and

K_M is always greater than 1, this may be concluded as the meandering model of Downstream Rotation Expansion Migration. The meander 18 in IR7 (Figure 3) reveals this model.

Constriction migration model

When the process of migrating laterally of the meandering channel slows down with the tendency of cut-off is beginning tardily near the bend inflections, and the curvature apex is approximately shifting with linear movement. The value of L_C, S, and R increases slowly, while the value of $|AX_{MB}|$, L_{ML}, and C relatively decrease. $\Delta\theta_U$ and $\Delta\theta_D$ remain constant, $\Delta\theta$ and $\Delta\theta'$ are basically maintained at 0°. K_M is always less than 1, this may be concluded as the meandering model of Symmetrical Constriction Migration. The meander 31 in IR10 (Figure 4)

reveals this model. When the process of migrating laterally of the meandering channel slows down with the tendency of cut-off is beginning tardily near the bend inflections, and the curvature apex is approximately shifting with the curvilinear movement towards the upstream.

The value of L_C, S, and R increases gradually, while the value of $|AX_{MB}|$, L_{ML}, and C relatively decrease. θ_U varies with the early increase and later decrease while θ_D with early decrease and later increase and then decrease; $\Delta\theta$ is positive while $\Delta\theta'$ is negative and both close to 0°. K_M is always less than 1, this may be concluded as the meandering model of Upstream Rotation Constriction Migration. The meander 2 in IR13 (Figure 4) reveals this model. When the process of migrating laterally of the meandering channel slows down with the tendency of cut-off is beginning tardily near the bend inflections, and the curvature apex is approximately shifting with the curvilinear movement towards the downstream.

The value of L_C, S, and R increases gradually, while the value of $|AX_{MB}|$, L_{ML}, and C relatively decrease. θ_U varies with early decrease and later increase and then decrease while θ_D with the early increase and later decrease; $\Delta\theta$ is negative while $\Delta\theta'$ is positive and both close to 0°. K_M is always less than 1, this may be concluded as the meandering model of Downstream Rotation Constriction Migration. The meander 1 in IR16 (Figure 4) reveals this model.

Composite Migration Model

The migration process of the meandering channel is accompanied by changes in topography, hydrodynamic, sedimentary environment and so on. Therefore, it is more inclined to see the complexes of the above 6 model in the nature channel. Basic composite models may be concluded as Symmetrical Expansion - Constriction Migration, Upstream Rotation Expansion - Constraint Migration, Downstream Rotation Expansion - Constriction Migration. Other more complex migration situations can be basically combined with these result.

Conclusion

This paper is to make a detailed characterization of the planform migration structure of meandering channels by making full use of the modern satellite images, and then in-depth analysis and discussion of the migration laws. A new set of new concrete and feasible characterization parameter for the meandering channel is put forward, and feasible forecasting model is extracted too. The research shows that the planform migration structure can be divided into 6 conventional and 3 basic composite models. Through different combinations, it can be used to describe and show the other migration structure.

The detailed description of the typical meanders on the 6 section of the Irtysh River has also been reflected in the migration structure. However, this paper also has some limitations, although the identify and research on the typical Irtysh River, it is still only the tip of the iceberg to the complex numbers of rivers in the world. Therefore, the methods and models in the study are still needed to be further extended in the after time.

REFERENCES

Asahi, K., Shimizu, Y. *et al*. 2013. Numerical simulation of river meandering with self-evolving banks. *Journal of Geophysical Research: Earth Surface* 118(4): 2208-2229.

Blum, M., Martin, J. *et al*. 2013. Paleovalley systems: Insights from Quaternary analogs and experiments. *Earth-Science Reviews* 116: 128-169.

Brice, J. C. 1974. Evolution of meander loops. Geological Society of America Bulletin 85(4): 581-586.

Debnath, J., Pan, N. D. *et al*. 2017. Channel migration and its impact on land use/land cover using RS and GIS: A study on Khowai River of Tripura, North-East India. *The Egyptian Journal of Remote Sensing and Space Science*.

Feng, Z. 2013. Chinese sedimentology (Second Edition). Beijing, Petroleum Industry Press.

Fryirs, K. A. 2017. River sensitivity: a lost foundation concept in fluvial geomorphology. *Earth Surface Processes and Landforms* 42(1): 55-70.

Ghinassi, M., Ielpi, A. *et al*. 2016. Downstream-migrating fluvial point bars in the rock record. *Sedimentary Geology* 334: 66-96.

Ghinassi, M., Nemec, W. *et al*. 2014. Plan—form evolution of ancient meandering rivers reconstructed from longitudinal outcrop sections. *Sedimentology* 61(4): 952-977.

Gilvear, D., Winterbottom, S. *et al*. 2000. Character of channel planform change and meander development: Luangwa River, Zambia. *Earth Surface Processes and Landforms* 25(4): 421-436.

He, Y. and Wang, W. 2008. Sedimentary rocks and sedimentary facies. Beijing, Petroleum Industry Press.

Hooke, J. 1980. Magnitude and distribution of rates of river bank erosion. *Earth Surface Processes and Landforms* 5(2): 143-157.

Hooke, J. 1984. Changes in river meanders: a review of techniques and results of analyses. *Progress in Physical Geography* 8(4): 473-508.

Hu, G., Chen, *et al*. F. 2017. Subdividing and comparing method of the fluvial facies reservoirs based on the complex sandbody architectures. *Petroleum Geology & Oilfield Development in Daqing* 36(2): 12-18.

Hu, G., Fan, T. *et al*. 2017. From Reservoir Architecture to Seismic Architecture Facies: Characteristic Method of a High-Resolution Fluvial Facies Model. *Acta Geographica Sinica* 91(2): 465-478.

Hu, H. 2016. Adjustment measures of remaining oil tapping based on sand body structure. *Lithologic Reservoirs* 28(4): 113-120.

Ielpi, A. and Ghinassi, M. 2014. Planform architecture, stratigraphic signature and morphodynamics of an exhumed Jurassic meander plain (Scalby Formation, Yorkshire, UK). *Sedimentology* 61(7): 1923-1960.

Jackson, R. G. 1976. Depositional model of point bars in the lower Wabash River. *Journal of Sedimentary Research* 46(3): 579-594.

Kasvi, E. 2015. Fluvio-morphological processes of meander bends-Combining conventional field measurements, close-range remote sensing and computational modelling. Ph.D. Thesis, University of Turku.

Kasvi, E., Laamanen, L. *et al*. 2017. Flow Patterns and Morphological Changes in a Sandy Meander Bend during a Flood—Spatially and Temporally Intensive ADCP Measurement Approach. Water 9(2): 106.

Lin, Z., Shan, J. *et al*. 2017. Meticulous Depiction and Genetic Mechanism of Unconformity Belt Structure. *Earth Science Research* 6(2): 19.

Ma, S., Sun, Y. *et al*. 2008. The Method for Studying Thin Interbed Architecture of Burial Meandering Channel Sandbody. *Acta Sedimentologica Sinica* 26(4): 632-639.

Mithun, D., Dabojani, D. *et al*. 2012. Evaluation of meandering characteristics using RS & GIS of Manu River. *Journal of Water Resource and Protection* 2012.

Mu, L. 2000. Stages and characteristic of reservoir description. Acta Petrolei Sinica 21(5): 103-108.

Nami, M. 1976. An exhumed Jurassic meander belt from Yorkshire, England. Geological Magazine 113(1): 47-52.

Schuurman, F., Kleinhans, M. G. *et al*. 2016. Network response to disturbances in large sand-bed braided rivers. *Earth Surface Dynamics* 4(1): 25-45.

Shan, J., Zhang, J. *et al*. 2015. Analysis of sedimentary and evolution process for underground meandering river point bar: a case study from No.23 thin layer of Yangdachengzi oil reservoir in Jilin oilfield. *Acta Petrolei Sinica* 36(7): 809-819.

Shi, S., Hu, S. *et al*. 2012. Building geological knowledge database based on Google Earth software. *Acta Sedimentologica Sinica* 30(5): 869-878.

Sui, X. 2006. A study on internal architecture of channel sand in meandering river, Northeast Petroleum University.

Willis, B. J. and Tang, H. 2010. Three-dimensional connectivity of point-bar deposits. *Journal of Sedimentary Research*, 80(5): 440-454.

Wu, C., Bhattacharya, J. P. *et al*. 2015. Paleohydrology and 3D facies architecture of ancient point bars, Ferron Sandstone, Notom Delta, south-central Utah, USA. *Journal of Sedimentary Research*, 85(4): 399-418.

Wu, C., Ullah, M. S. *et al*. 2016. Formation of point bars through rising and falling flood stages: Evidence from bar morphology, sediment transport and bed shear stress. Sedimentology 63(6): 1458-1473.

Wu, S. and Wang, Z. 1999. A new method of non-marine reservoir flow unit study. *Acta Sedimentologica Sinica* 17(2): 87-92.

Xu, J., Cai, G. *et al*. 2016. Research progress in river geomorphology in China: In memory of 100-year anniversary of Shen Yuchang's birth. *Acta Geographica Sinica* 71(11): 2020-2036.

Xue, P. 1991. An introduction to reservoir models of point bar facies. Beijing, Petroleum Industry Press.

Yin, T., Zhang, C. *et al*. 2001. Remaining oil distribution prediction based on high-resolution sequence stratigraphy. Petroleum Exploration and Development 28(4): 79-82.

Zhang, C., Zhang, S. *et al*. 2004. Advances in Chinese Fluvial Sedimentology from 1983 to 2003. *Acta Sedimentologica Sinica* 22(2): 183-192.

Zhu, X. 2008. Sedimentary petrology. Beijing, Petroleum Industry Press.

****